Application of a critical state model for the cyclic loading of sands

Reza Imam
Amirkabir University of Technology, Tehran, Iran
Dave Chan
University of Alberta, Edmonton, AB, Canada

ABSTRACT
A critical state constitutive model was developed at the University of Alberta with emphasis on capturing the main aspects of the behavior of loose liquefiable sands. The model, which has been presented in details in previous publications, was formulated and verified for monotonic loading of sands in different directions and shearing modes. However, considering the importance of sand liquefaction under cyclic loading and the need for constitutive model that can verifiably predict such phenomena, applicability of the model was later extended to cyclic loading. This paper presents the formulation that extends the model for cyclic loading. Considering the capped shape of the yield surface used in the model, bounding surface plasticity was found to be an appropriate modelling concept to take into account the effects of cyclic loading. Ability of the model to predict the behavior of granular soils subjected to cyclic loading is verified by comparing measured and predicted responses of sand in triaxial tests.

1. INTRODUCTION

The Critical State Soil Mechanics (CSSM) was first introduced as a theoretical framework for modelling the behavior of fine-grained soils (Roscoe et al., 1958). Due to the more complex dilatancy behavior of granular materials compared to clayey soils, the CSSM has been more successfully used for modelling the behavior of fine-grained soils for many years. However, over the past decade, modifications have been made to this framework, especially in dealing with sand dilatancy, in order to render it suitable for modelling the behavior of granular materials (see e.g. Jefferies, 1993; Crouch et al., 1994; Manzari and Dafalias, 1997).

One of the important advantages of using this framework is the ability to model the behavior of soils with different void ratios (densities) and confining pressures using the same model parameters. Therefore, it is not necessary to re-calibrate such models in order to predict the behavior of samples with different densities or confining pressures.

One of the important aspects of the behavior of granular soils is their response to cyclic loading. Many damages to structures constructed on or using granular materials are caused by loads that are cyclic or dynamic in nature. Examples of such damages are the liquefaction and lateral spreading of loose, saturated granular soils, and the seismic settlements of loose saturated and dry granular materials during an earthquake.. Modelling of the behavior of granular materials subjected to cyclic loading within the framework of CSSM is complicated, and the majority of the models developed for predicting the behavior of granular soils under cyclic loading are not formulated using the CSSM concept (see e.g. Pastor, et al., 1985; di Prisco et al, 1993)

It is beneficial, therefore, to develop constitutive models with ability to deal with cyclic loading in the CSSM framework. A number of models with using the CSSM concept have been presented recently (see e.g. manzari and Dafalias, 1997; Papadimitriou et al., 2001). However, the performance of these models in predicting sand behavior over a wide range of void ratios, confining pressures, and loading conditions is not known. In particular, the ability of a model to predict the behavior of loose and very loose sand subjected to various loading conditions should be verified such that it can reliably be used in the analysis of soil structures subjected to cyclic and earthquake loading.

In this paper a constitutive model that was previously developed in the framework of CSSM for predicting the behavior of granular soils over a wide range of void ratios, confining pressures, and loading directions under monotonic condition is extended to cyclic loading. The intention is to extend the monotonic model by introducing the least number of material parameters to the existing model to maintain its simplicity. The result is that only one material parameter is added. A brief summary of the existing model for monotonic loading is first presented, followed by the approach adopted to extend it to cyclic loading. Model predictions of the behavior of sands in cyclic loading are then compared with laboratory observations. Finally the performance of the model is discussed.

2. SUMMARY OF THE CONSTITUTIVE MODEL

A critical state constitutive model for sands has been developed with emphasis on taking into account important aspects of the behavior of loose liquefiable sand. Details of the model and its formulation are described by Imam et al. (2005), and the constitutive relationships are summarized in the Appendix of this paper. The model uses a capped yield surface with the stress ratio M_p at its point of peak deviatoric stress (q) obtained from the undrained effective stress path in triaxial tests.

In the model, stress-dilatancy is based on Rowe's (1962) dilatancy relationship combined with a modified form of the equation proposed by Manzari and Dafalias

(1997). The failure criterion is given by a friction angle that depends on the current state parameter (Been and Jefferies 1985) through a slightly modified version of a relationship suggested by Wood et al. (1994).

The model uses a single set of parameters to predict sand behavior over a wide range of void ratios and confining pressures. The critical state line represents the soil state at large strain, while the behavior at small and medium strains are captured by other material parameters such as the yielding, dilatancy, and plastic modulus parameters, which take into account anisotropy.

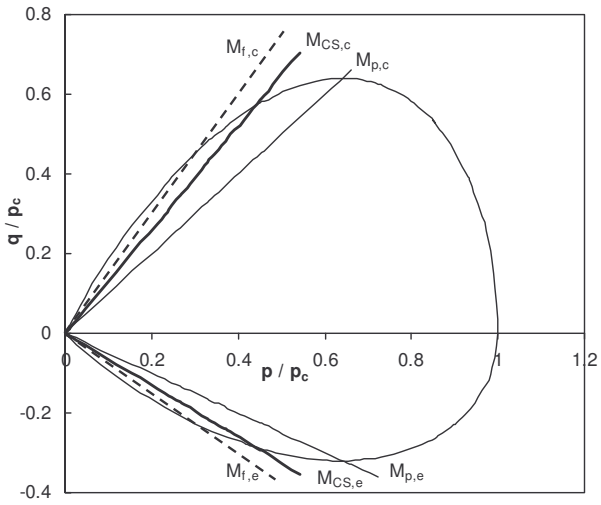

Figure 1 – Yield surface of isotropically consolidated sand

Figure 1 shows a graphical representation of the yield surface, and the stress ratios at critical state (M_{cs}) and at failure (M_f) in a p-q plane normalized to the maximum mean normal stress at yielding (p_c). Values of M_p in triaxial compression and triaxial extension are referred to as $M_{p,c}$ and $M_{p,e}$, respectively. These stress ratios control the yield surface shape (i.e. width), and account for the effects of void ratio, mean normal stress, and inherent anisotropy on the yielding stresses. A small M_p results in a slender yield surface and applies to sand that is loose, subjected to high confining pressures, or loaded in a weak direction such as the loading condition of a triaxial extension test.

Stress-induced anisotropy is represented by the stress ratio α, at which the tangent to the yield surface is parallel to the q-axis. This stress ratio is non-zero only in anisotropically consolidated sand. Size of the yield surface is determined by p_c.

3. MODELLING CYCLIC LOADING CONDITIONS

3.1 General

The two common approaches for modelling soil behavior in cyclic loading conditions is using kinematic hardening (Mroz, 1967) or the bounding surface plasticity (Dafalias and Herrman, 1982). The second appears to be more commonly used in recent years, likely due to its simpler formulations. In this method, the general framework for modelling the behavior of sand under monotonic loading can first be established, and an extension, including a mapping rule and plastic modulus for modelling unloading can then be introduced. The mapping rule relates the plastic modulus and strain increment direction during unloading to those of an image point on the bounding (yield) surface during loading. Therefore, plastic straining can occur during unloading, similar to that which takes place during loading, but the plastic modulus and strain increment direction may be different from (but often related to) those of loading. It is therefore convenient to extend formulations that can successfully model soil behavior in monotonic loading such that unloading can also be modelled using the same model elements used for monotonic loading. Such modifications have been applied in this paper to the constitutive model introduced by Imam et al. (2005).

3.2 General elastoplasticity relationships

The general elastoplasticity relationships can be found in most classical texts related to modelling. However, it was found convenient to use the following unit normal approach as introduced by Pastor, et al. (1985).

The relationship between an increment of stress, $\mathrm{d}\boldsymbol{\sigma}$, and an increment of strain, $\mathrm{d}\boldsymbol{\varepsilon}$, can be written in matrix form as follows:

$$\mathrm{d}\boldsymbol{\varepsilon} = \mathbf{C}\,\mathrm{d}\boldsymbol{\sigma} \qquad [1]$$

in which $\mathbf{C}$ is the constitutive matrix. The direction of the stress increment $\mathrm{d}\boldsymbol{\sigma}$ relative to the direction of the unit vector normal to the loading surface $\mathbf{n}_F$ determines whether loading or unloading occurs due to application of the stress increment. The constitutive matrix for loading and unloading are $\mathbf{C}_L$ and $\mathbf{C}_U$ respectively. Therefore:

$$\text{if} \quad \mathbf{n}_F\,\mathrm{d}\boldsymbol{\sigma} > 0: \qquad \mathrm{d}\boldsymbol{\varepsilon} = \mathbf{C}_L\,\mathrm{d}\boldsymbol{\sigma} \qquad [2a]$$

$$\text{if} \quad \mathbf{n}_F\,\mathrm{d}\boldsymbol{\sigma} < 0: \qquad \mathrm{d}\boldsymbol{\varepsilon} = \mathbf{C}_U\,\mathrm{d}\boldsymbol{\sigma} \qquad [2b]$$

Consistent with experimental observations, and as assumed in bounding surface plasticity, we assume that plastic strains develop during both loading and unloading. Therefore, the constitutive matrices in these cases can be determined from:

$$\mathbf{C}_L = \mathbf{C}^e + \mathbf{n}_{gL}\mathbf{n}_F / \mathrm{H}_L \qquad [3a]$$

$$\mathbf{C}_U = \mathbf{C}^e + \mathbf{n}_{gU}\mathbf{n}_F / H_U \quad [3b]$$

in which $\mathbf{n}_{gL}$ and $\mathbf{n}_{gU}$ are, respectively, the unit vectors normal to the plastic potential during loading and unloading; and, H_L and H_U are the corresponding plastic moduli.

It is noted that since the model presented by Imam et al. (2005) uses a non-associated flow rule for sands, the unit normal to the plastic potential surface and the loading surface are taken to be different in the expressions presented here.

The stress-strain relationships of the current model can now be obtained by substituting the unit normal to the yield and plastic potential surfaces, the elastic parameters, and the plastic moduli in Equations 1 to 3. However, in order to model cyclic loading, new variables are needed since they cannot be determined from the relationships provided for monotonic loading. These are the unit vector normal to the plastic potential surface during unloading, $\mathbf{n}_{gU}$, and the plastic modulus during unloading, H_U. Following the typical plasticity procedure, the plastic modulus for loading, H_L, can be determined using the model elements to satisfy the consistency condition.

3.3 Model stress-strain relationships

Relationships defining model elements are provided in the Appendix. These relationships can be used to determine the vectors and variables needed to obtain the stress-strain relationships given in Equations 1 to 3. In this section, these vectors and variables are determined for the triaxial test conditions, in which the stress (p, q) and strain (ε_p, ε_q) variables are defined as indicated in the notations section of this paper.

The unit normal to the yield surface is obtained from the following relationship:

$$\mathbf{n}_F = \left(\frac{\partial f}{\partial p} \quad \frac{\partial f}{\partial q}\right) \Big/ \left[\left(\frac{\partial f}{\partial p}\right)^2 + \left(\frac{\partial f}{\partial q}\right)^2\right]^{1/2} \quad [4]$$

in which:

$$\frac{\partial f}{\partial p} = \frac{M_\alpha{}^2}{2(pp_c)^{1/2}} - \frac{2}{p}\left(\eta^2 - \alpha\eta\right) \quad [5]$$

$$\frac{\partial f}{\partial q} = \frac{2}{p}\left(\eta - \alpha\right) \quad [6]$$

The unit normal to the plastic potential for loading and unloading conditions can be determined using the dilatancy relationship. If the components of $\mathbf{n}_g$ in the p and q directions are referred to as n_{gp} and n_{gq} respectively, the unit normal can be written in the following from:

$$\mathbf{n}_g = \left(n_{gp} \quad n_{gq}\right) \quad [7]$$

To obtain $\mathbf{n}_g$ for loading and unloading conditions, components consistent with loading and unloading should be used in Equation 7, respectively. For loading, these components are defined below:

$$n_{gp,L} = d/(d^2+1)^{1/2} \quad [8a]$$

$$n_{gq,L} = 1/(d^2+1)^{1/2} \quad [8b]$$

in which d is the sand dilatancy as defined in the Appendix. Since during unloading, the change in the absolute value of the shear strain increment is negative, a modification is needed when using the stress-dilatancy relationship. In this case (unloading), components of the unit normal to the plastic potential can be obtained from those used for loading, by applying the following modifications:

$$n_{gpU} = -\,|n_{gp,L}| \quad [9a]$$

$$n_{gq,U} = -n_{gp,L} \quad [9b]$$

The last step in completing the formulation involves the determination of the plastic modulus. For loading, this modulus, H_L, can be obtained by applying the consistency condition, which leads to the following relationship:

$$H_L = -\sqrt{\frac{2}{3}}\frac{df}{dp_c}\frac{dp_c}{d\boldsymbol{\varepsilon}_q} \quad [10]$$

in which:

$$\frac{df}{dp_c} = -\frac{M_\alpha{}^2}{2p_c}\left(\frac{p}{p_c}\right)^{1/2} \quad [11]$$

In the context of bounding surface plasticity, the plastic modulus for unloading is often obtained using a mapping rule, which relates the plastic modulus of the current stress state during unloading to the plastic modulus corresponding to the stress state on the mapped, the

image stress state on the bounding surface. In the current model, however, we use a simpler relationship in which the current plastic modulus in unloading is taken as a multiple of the current plastic loading modulus. This will introduce one additional model parameter (denoted by R_U as shown later) for modelling cyclic loading. It is possible to somewhat refine this relationship in order to achieve better predicted stress-strain relationship. However, this is not attempted here.

The ratio of the plastic modulus during unloading to that during loading is referred to as R_u here. Therefore:

$$H_U = R_U H_L \qquad [12].$$

4. MODELLING SAND BEHAVIOR IN CYCLIC LOADING

4.1 Drained sand behavior in cyclic loading

Figure 2 shows results of drained cyclic loading tests on Fuji River sand presented by Tatsuoka and Ishihara (1974). Fuji River sand has maximum and minimum void ratios of 1.08 and 0.53, respectively, and the test was carried out on a sample with a void ratio of 0.74, equivalent to a relative density of 62%. The sample was consolidated to a confining pressure of about 200 kPa and subjected to cyclic axial loading, which increased in amplitude in consecutive cycles.

Figure 2 (a) shows that during consecutive cycles of loading, the specimen continues to experience contraction as long as the stress ratio remains below a certain level. However, on the extension side, as the stress ratio exceeds this stress ratio level (referred as the phase transformation by Ishihara, 1975), the sample dilates upon further straining, and this dilation continues until the start of the next unloading cycle, which results in the resumption of contraction as in lower-stress-ratio cycles. It may also be noticed that unloading is always associated with contraction regardless of the stress ratio from which unloading starts.

Figure 2 (a) also shows that during loading on either the compression or extension sides, as the stress ratio reaches its higher ends, the rate of contraction with the change in stress ratio increases, and this increase continues until the next unloading is initiated.

Figure 2 (b) shows the changes in stress ratio q/p with shear strain for the same test. It shows that in low-stress-amplitude cycles, small strains are developed, and the changes in shear strain with stress ratio remaines almost similar throughout the loading/unload cycle. However, as the stress amplitude of the loading cycle is increased, the rate of development of the shear strain with the increase in stress ratio increases, especially at the higher stress ratios.

Figure 3 shows the predicted behavior of the sand in the test discussed. It shows that the main features of the behavior of Fuji River sand in this test, as discussed before, have been predicted reasonably well, considering that only one additional model parameter for modelling cyclic loading was used. However, it seems possible to improve the predictive capability of the model if the ratio of unloading to loading plastic moduli is made somewhat

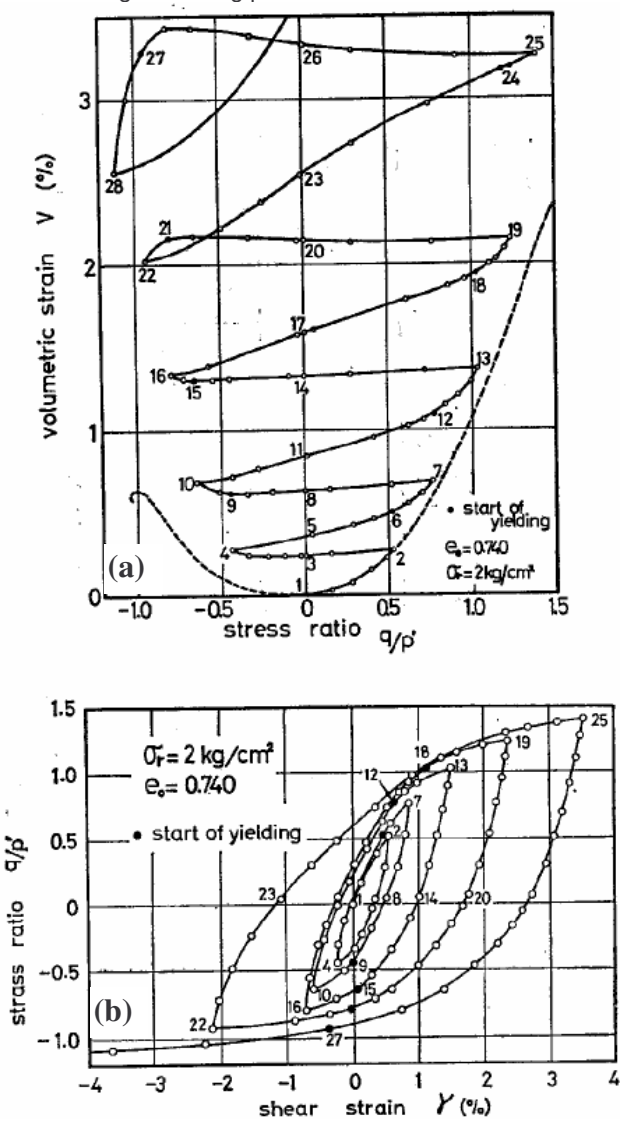

Figure 2 – Drained behavior of Fuji River sand during cyclic loading: (a) volumetric strain v.s. stress ratio (b) stress ratio v.s. shear strain (modified after Tatsuoka and Ishihara, 1974)

variable, for example a function of stress ratio or size of the yield surface.

4.2 Undrained sand behavior in cyclic loading

Figure 4 shows results of undrained stress-controlled cyclic loading tests on medium dense Nigata sand presented by Ishihara et al. (1975). As shown in this figure, application of the loading cycles to the sand sample resultes in the generation of pore pressures and movement of the stress path in the p-q plane towards the origin. This occurs due to the tendency of the sample to contract during the cyclic loading as observed in the drained test on Fuji River sand.

During the initial stress cycles, small shear strains are developed, and the shear stress-shear strain loop has a vertical shape as observed in Figure 4 (b). However, as the stress path moved closer to the origin of the p-q plane, shear strains develop at an accelerated rate and the stress-strain loop become increasingly more inclined, until it becomes almost completely horizontal in the last cycle.

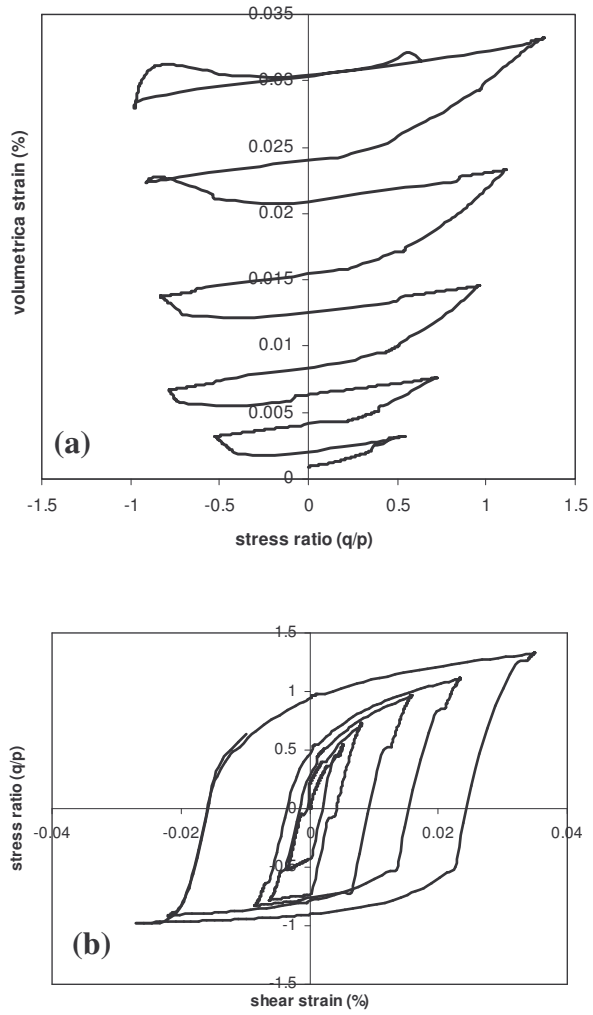

Figure 3 – Predicted behavior of Fuji River sand in cyclic loading: (a) volumetric strain v.s. stress ratio (b) stress ratio v.s. shear strain

These results were obtained from a stress-controlled test on medium dense sand. The behavior of looser Nigata sand is considered of more interest due to its greater potential for pore pressure generation and susceptibility to liquefaction.

Model prediction for the behavior of loose Nigata sand in strain-controlled loading is shown in Figure 5. It is shown that for this condition, the model also captures the main features of the sand behavior in undrained cyclic loading, including the generation of pore pressures and movement of the stress path towards the origin, and the gradual inclination of the stress-strain loop. Compared to the test result shown, this sample is looser and, as a result, the model predicts that the generation of pore pressure and inclination of the stress-strain loop occur at a greater rate, as expected, due to the higher contractive potential of this looser sample.

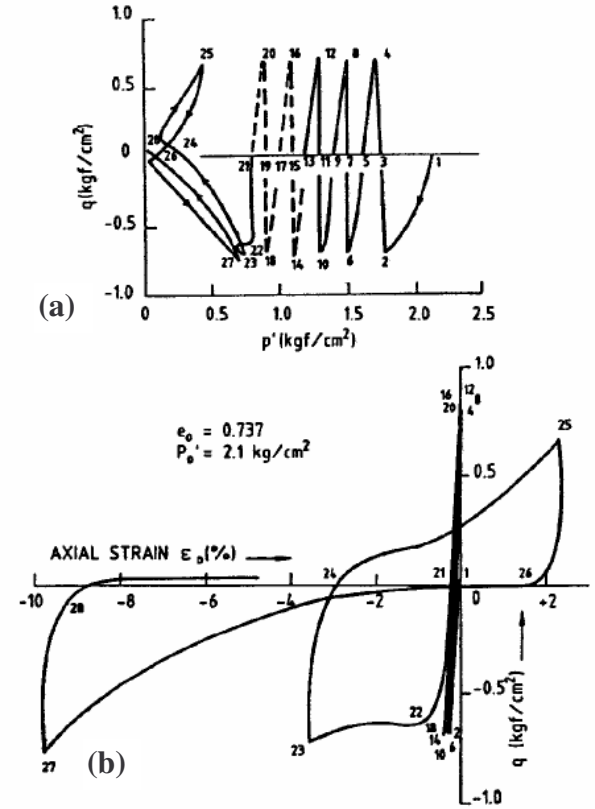

Figure 4 – Undrained behavior of Nigata sand in cyclic loading: (a) shear stress v.s. mean normal stress (b) shear stress v.s. shear strain (modified after Ishihara et al., 1975)

Table 1 – Model parameters

Parameter	Fuji River Sand	Nigata Sand
k_p	1.5	1.5
a_p	0.15	0.15
φ_μ	24	21
φ_{cv}	31	28
k_{PT}	1.25	1.25
a_{PT}	-0.08	0.15
k_f	0.75	0.75
h	1	1
G_r (kPa)	500	500
K_r (kPa)	800	850

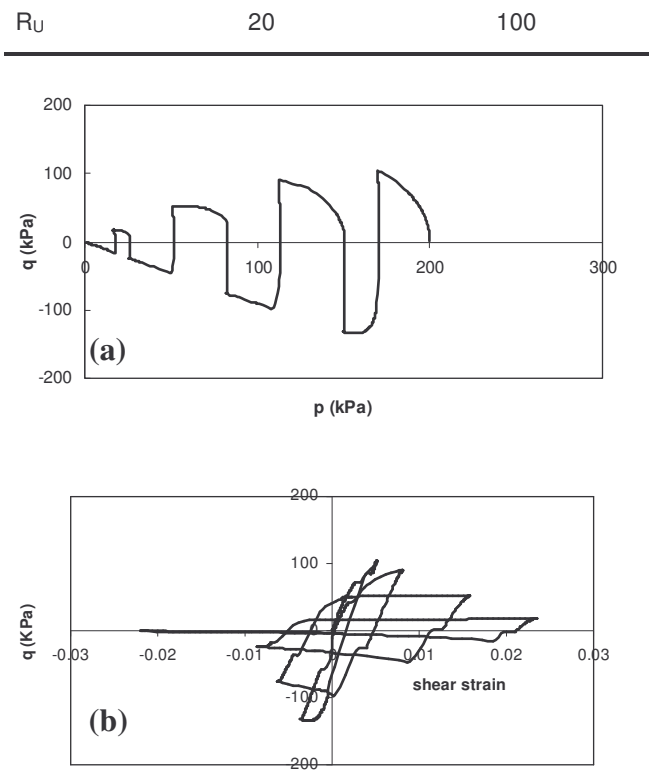

Figure 3 – Predicted undrained behavior of Nigata sand in cyclic loading: (a) shear stress v.s. mean normal stress (b) shear stress v.s. shear strain

Table 1 shows the model parameters used in modelling the behavior of Fuji River and Nigata sands.

5. COLCLUSIONS

A critical state constitutive model for monotonic loading of sands was extended for modelling cyclic loading using a simple procedure based on bounding surface plasticity. The extension adds only one model parameter to those needed for modelling monotonic loading. Comparisons of model predictions and observed behavior of sands show that the extended model can capture the main features of sand cyclic behavior in drained and undrained conditions. However, some improvements in the predictive capability of the model may be achieved by defining a more refined plastic modulus during unloading.

REFERENCES

Been, K. and Jefferies, M. G. 1985. A state parameter for sands. Geotechnique, **35**(2): 99-112

Crouch, R. S., Wolf, J., and Dafalias, Y. 1994. Unified critical state bounding surface plasticity model for soil. J.Eng.Mech., 120(11): 2251-2270.

Dafalias, Y. and Herrmann, L. R. 1982. Bounding Surface Formulation of Soil Plasticity. Chapter 10 in Pande, G.N.and Zienkiewicz, O.C.(eds.) Soil Mechanics-Cyclic and Transient Loads, Wiley: 253-282.

di Prisco, C., Nova, R., and Lanier, J. 1993. A mixed isotropic kinematic hardening constitutive law for sand. Modern approaches to plasticity ed.D.Kolymbas, Roterdam: Balkema.: 83-124.

Imam, S. M. R., Morgenstern, N. R., Robertson, P. K., and Chan, D. H. 2005. A Critical State Constitutive Model for Liquefiable Sand, Canadian Geotechnical Journal, 42: 830-855.

Ishihara, K., Tatsuoka, F., and Yasuda, S. 1975. Undrained deformation and liquefaction of sand under cyclic stresses. Soils and Foundation, **15**(1): 29-44.

Jefferies, M. G. 1993. Nor-Sand: a simple critical state model for sand. Geotechnique, 43(1): 91-103.

Manzari, M. T. and Dafalias, Y. F. 1997. A critical state two-surface plasticity model for sands. Geotechnique, 47(2): 255-272.

Mroz, Z. 1967. On the Description of Anisotropic Hardening. Journal of Mechanics and Physics of Solids, 15: 163-175.

Papadimitriou, A, G., Bouckovalas, G. D., and Dafalias, Y. 2001. Plasticity model for sand under small and large cyclic strains. J. of Geotechnical and Geoenvironmental Engineering, ASCE, 127(11): 973-983.

Pastor, M., Zienkiewicz, O. C., and Leung, K. H. 1985. Simple model for transient soil loading in earthquake analysis. II. Non-associative model for sands. Int.J.Num.Anal.Meth.Geomech., 9: 477-498.

Roscoe, K. H., Schofield A.N., and Wroth, C. P. 1958. On the yielding of soils. Geotechnique, 8(1): 22-53.

Rowe, P. W. 1962. The stress-dilatancy relation for static equilibrium of an assembly of particles in contact. Pro.of the Roy.Soc.A269: 500-527.

Tatsuoka, F., and Ishihara, K. 1974. Drained deformation of sand under cyclic stresses reversing direction. Soils and Foundations. 14(3): 51-65.

Wood, D. M., Belkheir, K., and Liu, D. F. 1994. Strain softening and state parameter for sand modelling. Geotechnique, 44(2): 335-339.

APPENDIX

The yield surface is defined using the following equation:

$$f = (\eta - \alpha)^2 - M_\alpha^2 \left[1 - \left(\frac{p}{p_c}\right)^{\frac{1}{2}}\right] = 0 \qquad [A\text{-}1]$$

$$M_\alpha^2 = (5M_p - \alpha)(M_p - \alpha) \qquad [A\text{-}2]$$

in which, for triaxial compression (TC) and triaxial extension (TE) we have:

$$M_{p,c} = \frac{6\sin\varphi_{p,c}}{3 - \sin\varphi_{p,c}} \quad \text{in TC} \qquad [A\text{-}3a]$$

$$M_{p,e} = \frac{6\sin\varphi_{p,e}}{3+\sin\varphi_{p,e}} \quad \text{in TE} \quad [A\text{-}3b]$$

and $\varphi_{p,c}$ and $\varphi_{p,e}$ are the friction angles at the point of peak q in TC and TE, respectively, and are obtained from:

$$\sin\varphi_{p,c} = \sin\varphi_\mu - k_p\,\psi \quad \text{in TC} \quad [A\text{-}4a]$$

$$\sin\varphi_{p,e} = \sin\varphi_\mu - k_p\,\psi - a_p \quad \text{in TE} \quad [A\text{-}4b]$$

in which φ_μ is the friction angle corresponding to $\psi_p = 0$ in TC and is typically close to the inter-particle friction angle of the sand; k_p and a_p are material parameters, and ψ is the state parameter. A Mohr-Coulomb type failure criterion, expressed in the following form, is used:

$$\sin\varphi_f = \sin\varphi_{cs} - k_f\,\psi \quad [A\text{-}5]$$

in which φ_{cs} is the critical state friction angle and k_f is a material parameter which is taken to be 0.75 for sand loaded in both TC and TE. Friction angles obtained from [6] are converted to equivalent stress ratios at failure $M_{f,c}$ and $M_{f,e}$ for TC and TE as in [3]. These are the maximum stress ratios attainable at the current soil state, and may not be equal to the current stress ratio η. It is only at critical state ($\psi = 0$) where the current and failure stress ratios coincide and we have $\eta = M_f = M_{cs}$. The flow rule is determined from the following relationship:

$$d = \frac{d\varepsilon_p^{\,p}}{d\varepsilon_q^{\,p}} = A\,(M_{cs}-\eta) \quad [A\text{-}6]$$

in which:

$$A_c = 9/(9 - 2M_{PT,c}\eta + 3M_{PT,c}) \quad \text{in TC} \quad [A\text{-}7a]$$
$$A_e = 9/(9 - 2M_{PT,e}\eta - 3M_{PT,e}) \quad \text{in TE} \quad [A\text{-}7a]$$

and $M_{PT,c}$ and $M_{PT,e}$, are obtained using the following relationships:

$$\sin\varphi_{PT,c} = \sin\varphi_{cs} + k_{PT}\,\psi \quad \text{for TC} \quad [A\text{-}8a]$$

$$\sin\varphi_{PT,e} = \sin\varphi cs + a_{PT} + k_{PT}\,\psi \quad \text{for TE} \quad [A\text{-}8b]$$

Hardening during shearing is determined from:

$$\frac{\partial p_c}{\partial \varepsilon_q^{\,p}} = \frac{hG}{(p_f - p_c)_{ini}}(p_f - p_c) \quad [A\text{-}9]$$

in which h is a non-dimensional material parameter related to soil stiffness during shearing, G is the elastic shear modulus, and $(pf - pc)_{ini}$ is the initial value of $(p_f - p_c)$ at the end of consolidation and prior to shearing. The value of p_f is obtained by substituting the current M_f for η in Equation [1]. Elastic moduli are defined as follows:

$$G = G_r\,\frac{(2.973-e)^2}{1+e}(p/p_a)^{1/2} \quad [A\text{-}10a]$$

$$K = K_r\,\frac{(2.973-e)^2}{1+e}(p/p_a)^{1/2} \quad [A\text{-}10b]$$

in which G_r and K_r are reference values that depend on the units used and may be obtained from the elastic moduli corresponding to the atmospheric pressure p_a.

NOTATION:

a_p, a_{PT}: Difference between $\sin\varphi$ at peak point of the yield surface and at PT in TC and TE, respectively
d,: Soil dilatancy
e, e_{cs}: current and critical state void ratios, respectively
f : Yield function
G, G_a: Elastic shear modulus at current and atmospheric mean normal stresses, respectively
h : Material parameter related to plastic shear stiffness
K, K_r : Elastic and reference bulk moduli, respectively
$K_0 = \sigma_h / \sigma_v$ Coefficient of lateral earth pressure
k_p, k_f, k_{PT} : Slope of variation of $\sin\varphi_p$, $\sin\varphi_f$ and $\sin\varphi_{PT}$ with state parameter, respectively
M_{cs}, $M_{cs,c}$, $M_{cs,e}$: Stress ratios q/p at critical state, and its values in TC and TE, respectively
M_p, $M_{p,c}$, $M_{p,e}$: Stress ratio at the peak point of the yield surface, and its values in TC and TE, respectively
M_μ, M_f: Stress ratio q/p corresponding to inter-particle friction and failure, respectively.
p, p_a, p_c, p_p, p_f : Effective mean normal stress ($= \sigma_1 + 2\sigma_3)/3$, and its values at atmospheric pressure and at consolidation, respectively.
q : Deviatoric stress ($=\sigma_1-\sigma_3$)
α : Stress ratio q/p at which tangent to yield surface is perpendicular to the p-axis
ε_1 , ε_3 : Major and minor principal strains respectively
ε_p , ε_q, $\varepsilon_p^{\,p}$, $\varepsilon_q^{\,p}$: Volumetric ($\varepsilon_p = \varepsilon_1 + 2\varepsilon_3$)and shear ($\varepsilon_q = 2(\varepsilon_1 - \varepsilon_3)/3$) strains and their plastic components, respectively
φ_f : Mobilized friction angle at failure
φ_{PT}, $\varphi_{PT,c}$, $\varphi_{PT,e}$: Friction angle at PT, and its values in TC and TE, respectively
φ_p, $\varphi_{p,c}$, $\varphi_{p,e}$: Friction angle at peak point of the yield surface, and its values in TC and TE, respectively

φ_μ, φ_{cv} : Inter-particle and constant volume friction angles, respectively

ψ: State parameter = $e - e_{cs}$